A. Supplementary Figures

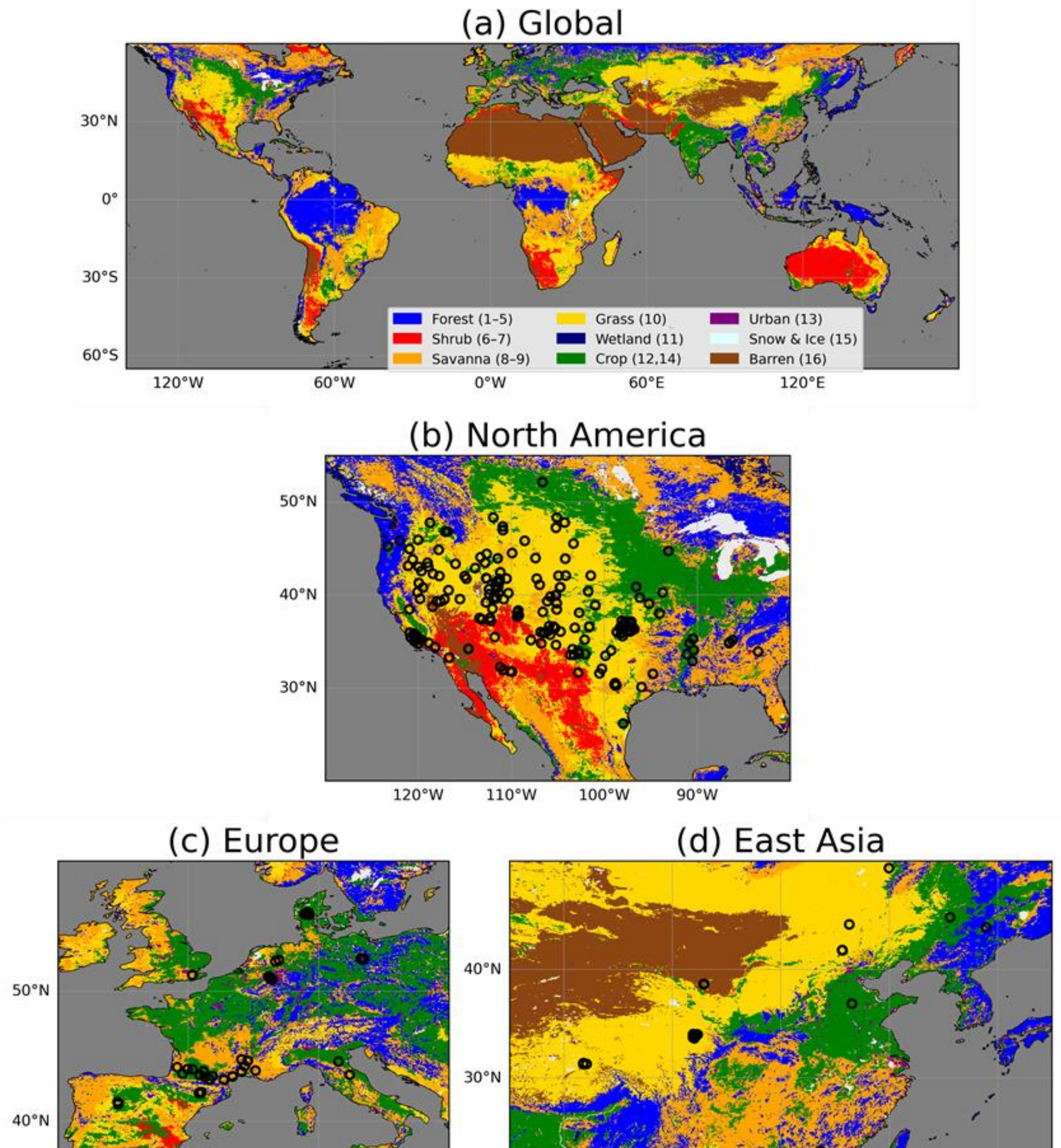

Figure S1: Climatological land cover classes from MODIS for 2001-2017. Panels (a-d) show the land cover over the globe, North America, Europe, and East Asia, respectively. "Forest" consists of IGBP classes 1-5, "Shrub" consists of IGBP classes 6-7, "Savanna" consists of IGBP classes 8-9, "Grassland" consists of IGBP class 10, "Wetland" consists of IGBP class 11, "Crop" consists of IGBP classes 12 & 14, "Urban" consists of IGBP class 13, "Snow and ice" consists of IGBP class 15, and "Barren" consists of IGBP class 16. Black circles represent in-situ observation stations used for validation.

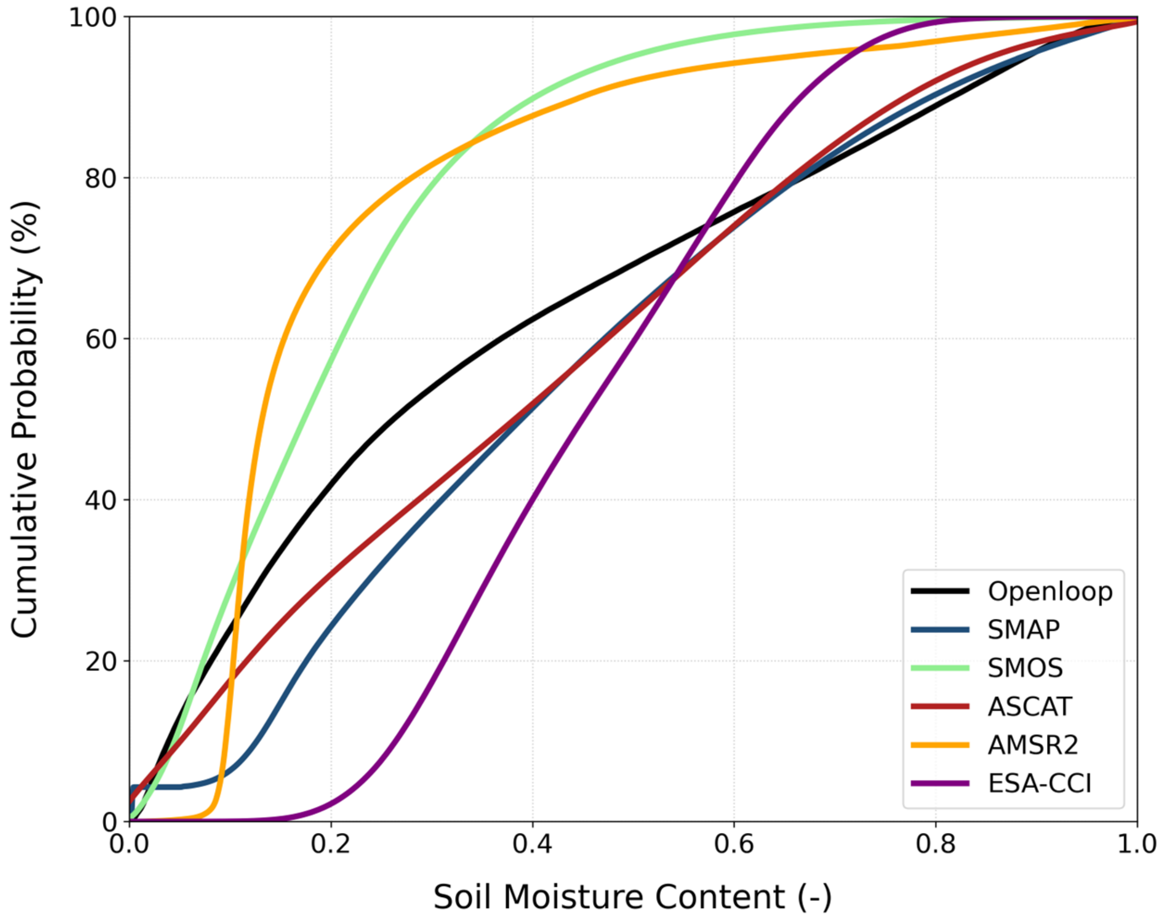

Figure S2: Cumulative distribution function (CDF) of surface soil moisture content as a fraction of saturation from SMAP, SMOS, ASCAT, AMSR2, and ESA-CCI retrievals and from the LSM Openloop simulation over North America (130°–75°W, 25°–50°N). The CDF for SMAP is computed for April 2015–September 2021. The CDFs for the other datasets are computed for January 2010–September 2021.

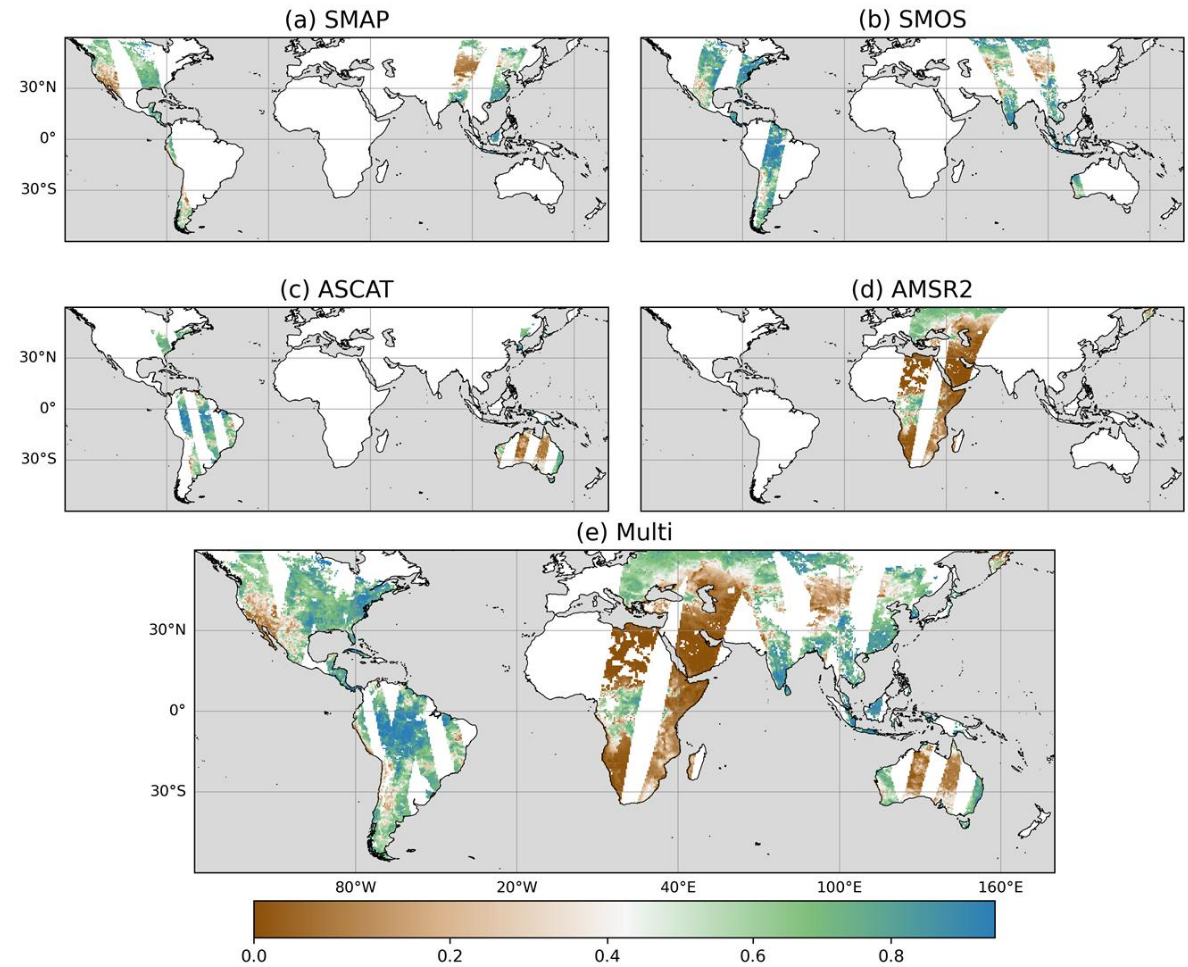

Figure S3: Spatial distribution of assimilated soil moisture observations from (a) SMAP, (b) SMOS, (c) ASCAT, (d) AMSR2, and (e) all sensors for the 2 May 2015, 21:00 UTC to 3 May 2015, 00:00 UTC assimilation window. Shading indicates rescaled moisture content of the surface soil layer as a fraction of saturation) (-).

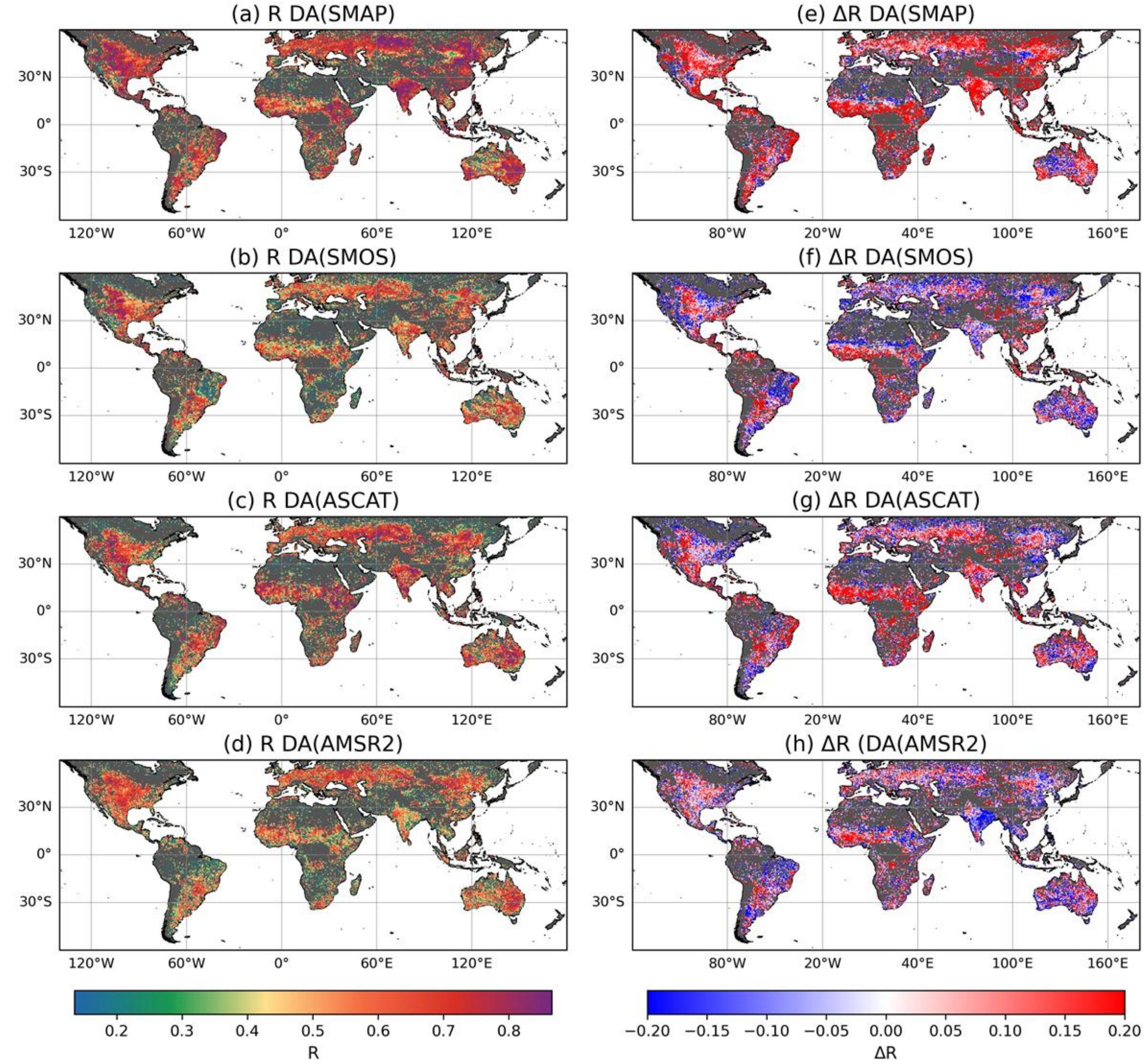

Figure S4: Anomaly temporal correlation (R; dimensionless) of daily surface SM for the single-sensor DA simulations (left column): (a) DA(SMAP), (b) DA(SMOS), (c) DA(ASCAT), and (d) DA(AMSR2). Skill improvement (ΔR) from single-sensor assimilation over the Openloop simulation (right column): (e) DA(SMAP), (f) DA(SMOS), (g) DA(ASCAT), and (h) DA(AMSR2).

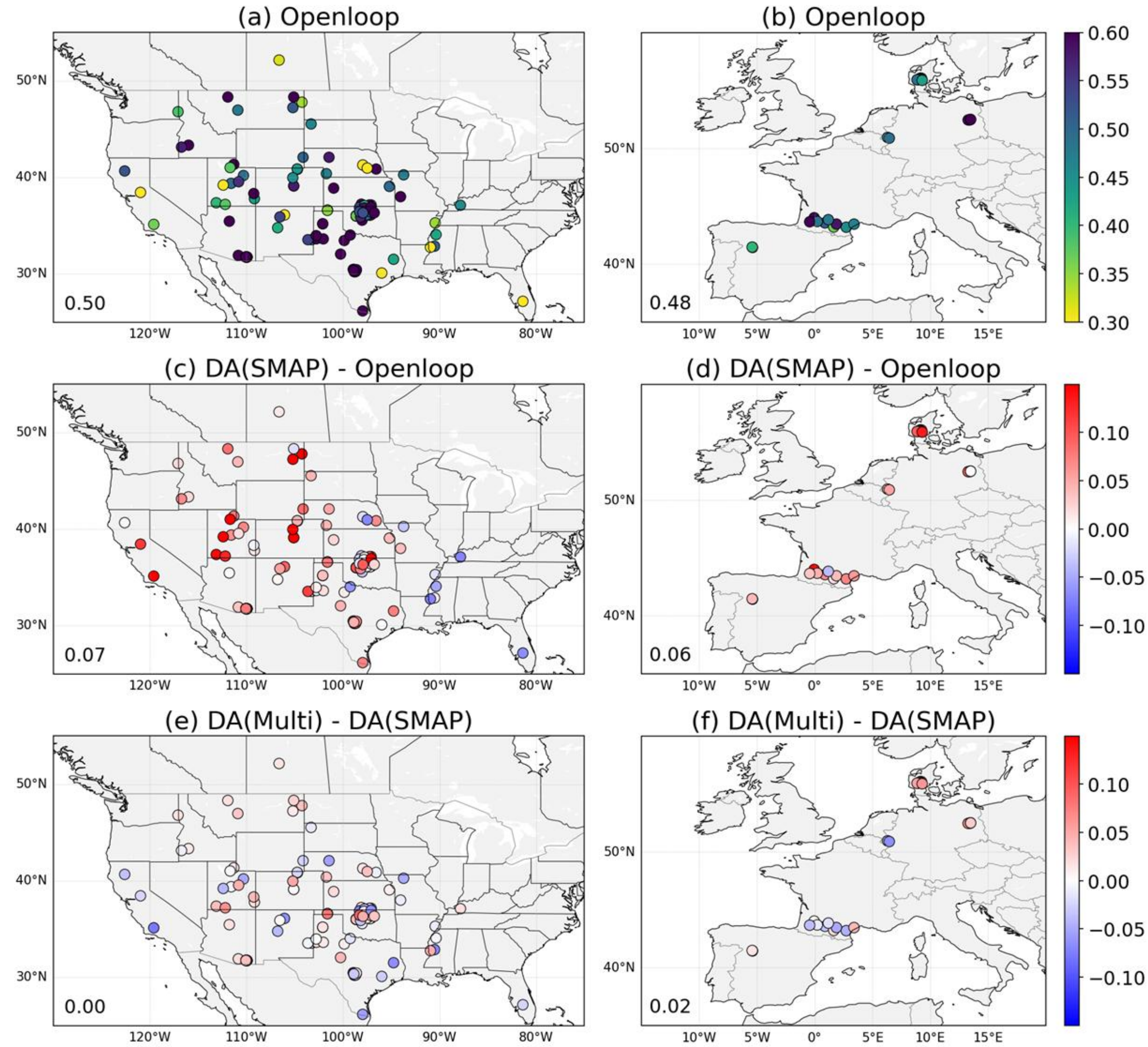

Figure S5: Temporal correlation coefficient of the anomaly time series (R; dimensionless) of surface SM estimates at in-situ sites from the Openloop simulation over (a) North America (N=163) and (b) Europe (N=35). (c-d) Difference in R between DA(SMAP) and Openloop. (e-f) Difference in R between DA(Multi) and DA(SMAP). The spatially averaged values are denoted in the lower-left corner of each panel. This figure shows the results on the daily time scale using only the station used in the sub-daily analysis.

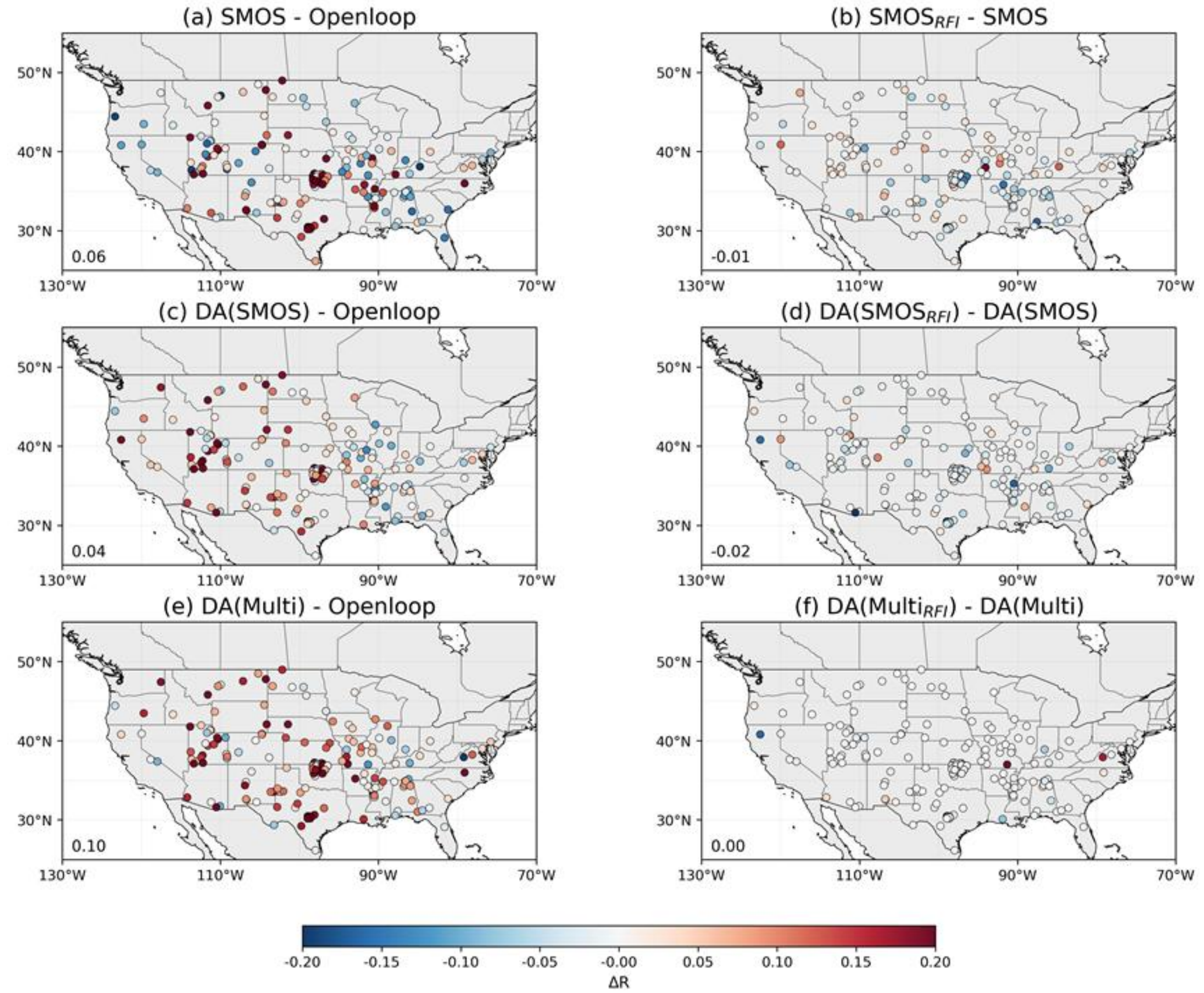

Figure S6: Surface soil moisture skill differences (ΔR; dimensionless) relative to the Openloop simulation at in-situ stations over North America (N=241) during April – September 2021. (a) and (b) represent the satellite retrieval skills of SMOS without RFI filtering and the difference between the unfiltered and filtered cases (using only data with RFI < 10%), respectively. (c) and (d) are the same as (a) and (b) but after single-sensor DA with SMOS. (e) and (f) are the same as (c) and (d) but for multi-sensor DA. Spatially averaged ΔR values are shown in the lower corner of each panel.

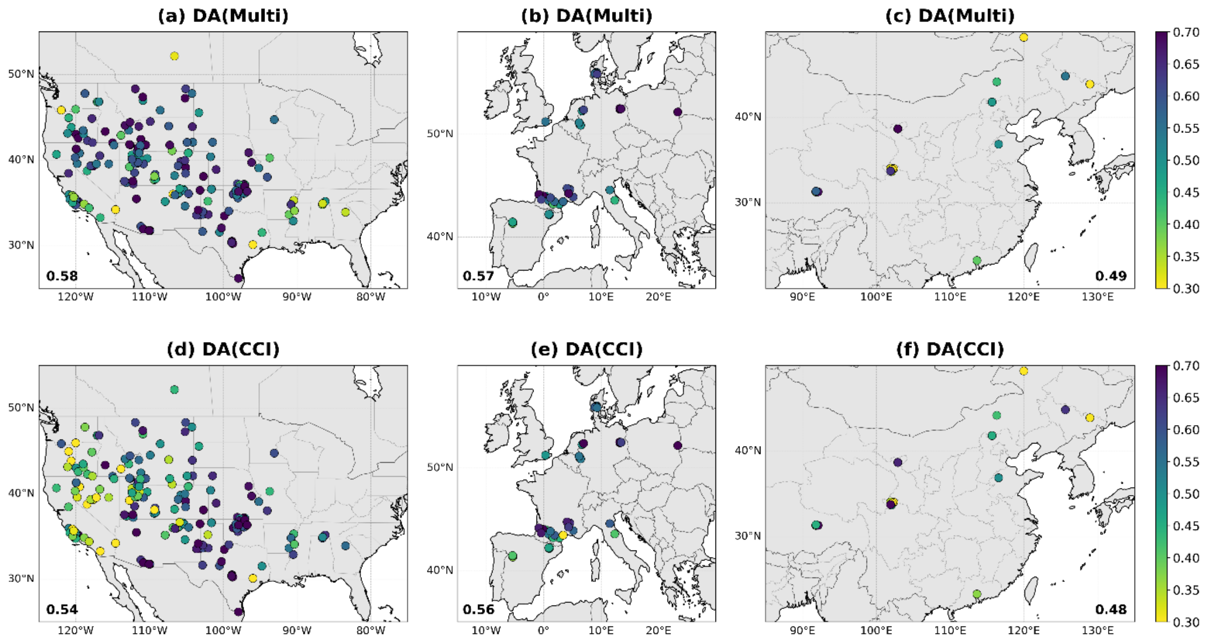

Figure S7: Surface soil moisture anomaly skill (R; dimensionless) at in-situ stations over North America during April – September, 2015-2021 for (a) – (c) DA(Multi) and (d) – (f) the ESA-CCI v09.2 product. Spatially averaged R values are shown in the lower corner of each panel.

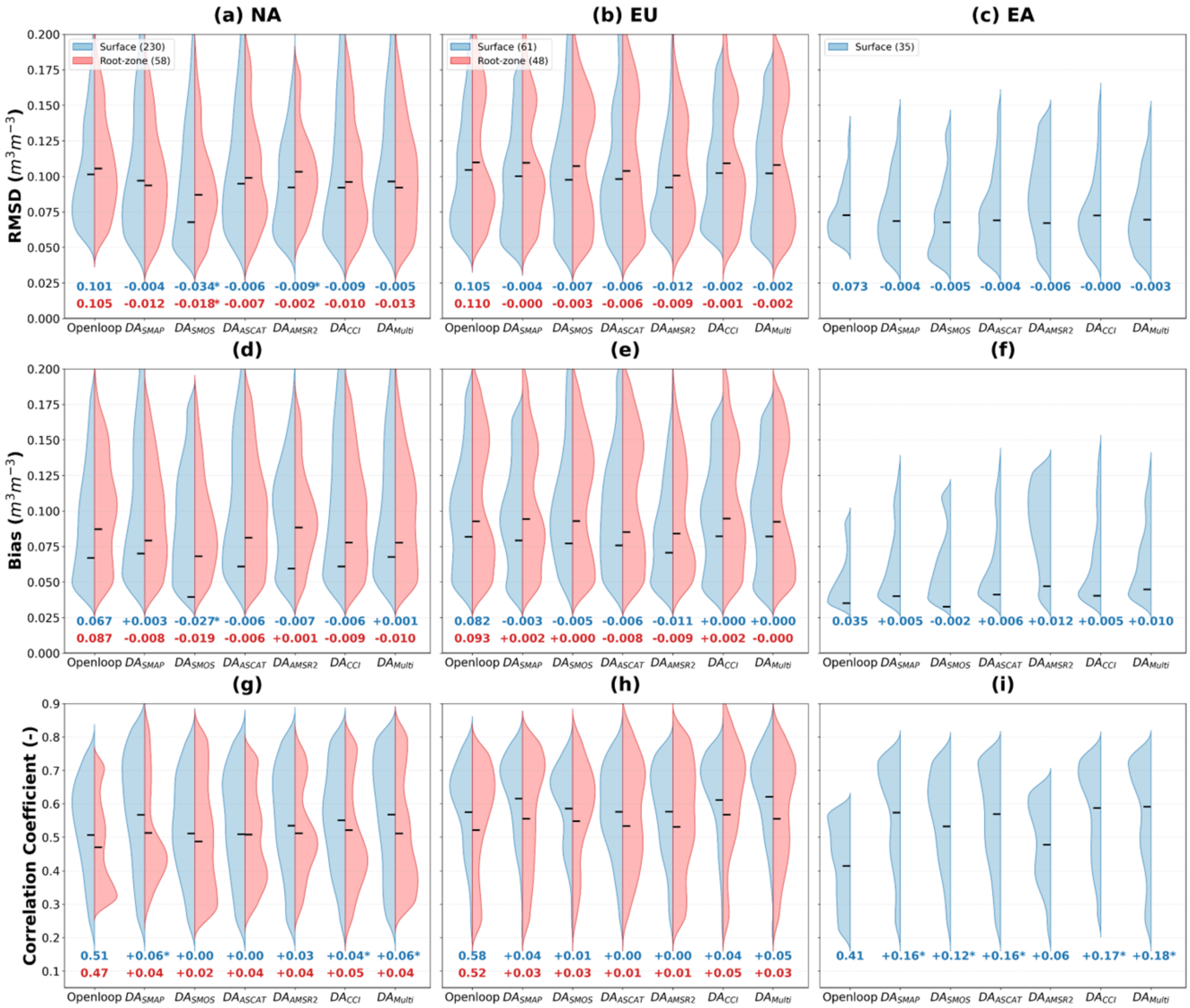

Figure S8: Same as Figure 4, but for (a)-(c) RMSE (m3 m-3), (d)-(f) Bias (m3 m-3), and (g)-(i) the correlation coefficient (-) of raw estimates, without removing the mean seasonal cycle.

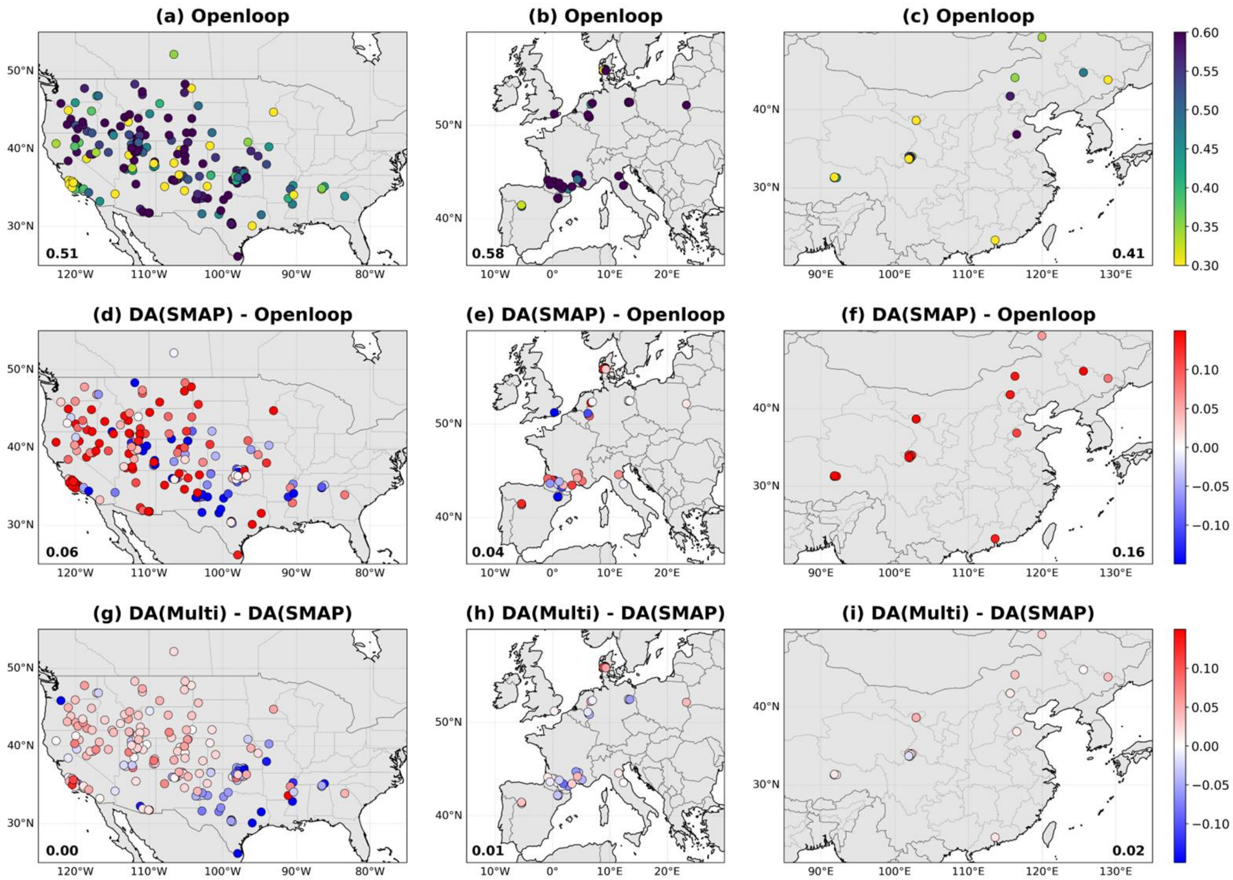

Figure S9: Same as Figure 3, but for the correlation coefficient of raw estimates without removal of the mean seasonal cycle.

Table S1. Details of the International Soil Moisture Network (ISMN) datasets over North America, Europe, and East Asia used in this study, including country, observation period, number of stations, measurement depth, and reference. All listed networks are used for daily scale analysis. Networks highlighted in orange provide hourly observations and are used for sub-daily assessment, while unshaded networks provide data only at the daily scale.

NETWORK	Country	Data availability (YYYY-MM-DD)	Number of stations	Depth (m)	Official References in ISMN (https://ismn.earth/en/)
ARM	USA	1993-06-29 to present	35	0.02-1.75	Cook et al., 2016
Berlin	Germany	2019-11-02 to present	23	0.05-0.85	The work of Martin Schreiner and the Berlin network team
COSMOS	USA	2008-04-28 to 2020-03-29	109	0.00-0.90	Zreda et al., 2008
HOBE	Denmark	2009-09-08 to 2019-03-13	32	0.00-0.55	Jensen et al., 2018
MAQU	China	2008-05-13 to 2019-06-01	27	0.05	Dente et al., 2012
NAQU	China	2010-06-15 to 2019-09-12	11	0.05	Dente et al., 2012
NGARI	China	2010-07-21 to 2019-09-10	23	0.05	Dente et al., 2012
REMEDHUS	Spain	2005-03-15 to 2025-01-01	24	0.00-0.05	Gonzalez-Zamora et al., 2018
RISMA	Canada	2013-04-24 to 2020-03-25	24	0.00-1.50	Ojo et al., 2015
SCAN	USA	1996-08-15 to present	222	0.05-1.42	Schaefer et al., 2007
SMOSMANIA	France	2007-01-01 to 2025-01-01	22	0.05-0.30	Calvet et al., 2016
PBO-H2O	USA	2004-09-27 to 2017-12-16	163	0.00-0.50	Larson et al., 2008
SOILSCAPE	USA	2011-08-03 to present	224	0.04-0.90	Moghaddam et al., 2016
SONTE-China	China	2020-12-31 to 2022-12-31	20	0.05	Li et al., 2022
TERENO	Germany	2009-12-31 to 2025-07-07	5	0.05-0.50	Bogena et al., 2018
TWENTE	Netherlands	2008-11-12 to 2020-12-31	44	0.05-0.80	Velde et al., 2023
TxSON	USA	2014-10-01 to 2022-11-08	41	0.05-0.05	Caldwell et al., 2019
USCRN	USA	2000-11-15 to present	115	0.05-1.00	Bell et al., 2013

Table S2. Details of SMAP, SMOS, ASCAT, and AMSR2 soil moisture datasets.

Soil Moisture Dataset	Dataset version	Microwave band (frequency)	Data type	Sampling depth	Units of data	Temporal coverage	Spatial resolution (posting)	Observation error
SMAP	V5, (DOI:10.5067/R50VUC07OM4W)	L-band (1.4 GHz)	Passive	~5 cm	($m^3\ m^{-3}$)	2015-present	36 km	0.04 $m^3\ m^{-3}$
SMOS	V700, (DOI:10.57780/SM1-857c3d7)	L-band (1.4 GHz)	Passive	~5 cm	($m^3\ m^{-3}$)	2010-present	36 km	0.08 $m^3\ m^{-3}$
ASCAT	V5.0 (DOI:10.15770/EUM_SAF_H_0006)	C-band (5.3 GHz)	Active	~2 cm	(%) (saturation ratio of soil moisture)	2007-present	25 km	10 %
AMSR2	V001 (DOI:10.5067/KZ9OOIENUO0C)	C-band (7.3 GHz)	Passive	~2 cm	($m^3\ m^{-3}$)	2012-present	10 km	0.08 $m^3\ m^{-3}$
ESA-CCI	V09.2 (DOI:10.5281/zenodo.19565425)	Multiple frequencies	Active & passive	~5 cm	($m^3\ m^{-3}$)	1979 – 2024	25 km	0.025 $m^3\ m^{-3}$

B. Single Instrumental Variable Method

This study evaluates the performance of surface soil moisture in single-sensor data assimilation (DA) experiments using the Instrumental Variable (IV) approach (Su et al., 2014) at a global scale. The IV approach is rooted in the concept of Triple Collocation Analysis (TCA), which is widely used for quantifying errors and uncertainties in soil moisture estimation (Stoffelen, 1998). While TCA requires three independent datasets—such as a satellite, a model, and in-situ observations—IV offers greater flexibility by requiring only two independent datasets, such as a satellite and a model. This makes it a valuable tool for evaluating data assimilation experiments where the assimilated datasets cannot be used for verification against in-situ data at a global scale. In our study, we construct a triplet for skill estimation that is composed of model output (DA), an independent satellite dataset not assimilated in each single-sensor experiment, and a 2-day lagged version of the same independent satellite dataset. The lagged dataset serves as an instrumental variable by exploiting the temporal persistence of soil moisture, where values remain correlated, but errors are not. While a 1-day lag provides a slightly stronger correlation with the soil moisture signal, a 2-day lag offers a higher degree of statistical independence. This is because satellite measurement errors can exhibit short-term autocorrelation, which a 2-day lag helps to eliminate. By prioritizing the core assumption of the IV method—that errors are uncorrelated—the use of a 2-day lagged dataset ensures a more stable and reliable analysis, despite a minor reduction in signal correlation (Fox et al., 2025; Dong et al., 2019). The performance improvement of single-sensor DA experiments is then evaluated using this IV approach, with the enhancement assessed globally relative to the Openloop simulation. For DA experiments using L-band observations (DA(SMAP) and DA(SMOS)), the IV sets were constructed using ASCAT as the reference satellite. Conversely, for C-band-based DA experiments (DA(ASCAT) and DA(AMSR2)), the IV sets were constructed using SMAP as the reference. The Openloop simulation was evaluated individually against each of the four satellite observations, and the results were averaged to serve as the baseline for assessing the performance of the DA experiments. Our global skill assessment is similarly applied only to anomaly time series, which removes the monthly mean of the SM estimates.

Covariance and IV Notation

In Triple collocation analysis (Stoffelen, 1998), three independent observation systems measuring the same geophysical variable are used to estimate random errors. By assuming that the errors are mutually uncorrelated and that each measurement is linearly related to the truth, TCA provides unbiased error variance estimates without requiring knowledge of the true value, and the truth-product correlations (R) can be solved (McColl et al., 2014). In the IV approach, as noted above, the satellite and the lag-2 time series of the satellite can provide the product error using only two independent products. The covariance between products x (in our case, satellite soil moisture observations) and y (model experiment surface soil moisture) with the true geophysical signal (true surface soil moisture) P is given by:

$$C_{xy} = a_x a_y C_{pp} \quad (1)$$

$$C_{xx} = a_x^2\, C_{pp} + \sigma_x^2 \quad (2)$$

$$C_{yy} = a_y^2\, C_{pp} + \sigma_y^2 \quad (3)$$

where, C_{xy} is the covariance between x and y, C_{xx} is the variance of x, C_{pp} is the variance of the true signal P, a_x is scaling factors for x, and σ_x^2 is error variances of x.

$$C_{Ix} = a_x^2 L_{pp} \quad (4)$$

L_{pp} is the lagged auto-covariance of the true signal. Using a lagged version of x as the instrumental variable I (in our cases, 2-day lagged time series of satellite soil moisture observations), the covariance relationships are C_{Ix} (Dong et al., 2019)

$$S_{ivs} \equiv \frac{C_{Ix}}{C_{Iy}} = \frac{a_x}{a_y} \quad (5)$$

where S_{ivs} is the IVs-estimated scaling ratio of the two products

$$\sigma_x^2 = C_{xx} - C_{xy} S_{ivs} \quad (6)$$

$$\sigma_y^2 = C_{yy} - \frac{C_{xy}}{S_{ivs}} \quad (7)$$

and their correlation with truth can be estimated as:

$$R_{Px}^2 = \frac{C_{xy}S_{ivs}}{C_{xx}} \quad (8)$$

$$R_{Py}^2 = \frac{C_{xy}}{C_{xx}S_{ivs}} \quad (9)$$

References on supplementary material

Dong, J., Crow, W. T., Duan, Z., Wei, L., and Lu, Y.: A double instrumental variable method for geophysical product error estimation, Remote Sensing of Environment, 225, 217–228, https://doi.org/10.1016/j.rse.2019.03.003,2019.

McColl, K. A., Vogelzang, J., Konings, A. G., Entekhabi, D., Piles, M., and Stoffelen, A.: Extended triple collocation: Estimating errors and correlation coefficients with respect to an unknown target, Geophysical Research Letters, 41, 6229–6236, https://doi.org/10.1002/2014GL061322, 2014.

Stoffelen, A.: Toward the true near-surface wind speed: Error modeling and calibration using triple collocation, Journal of Geophysical Research: Oceans, 103, 7755–7766, https://doi.org/10.1029/97JC03180, 1998.

Su, C.-H., Ryu, D., Crow, W. T., and Western, A. W.: Beyond triple collocation: Applications to soil moisture monitoring, Journal of Geophysical Research: Atmospheres, 119, 6419–6439, https://doi.org/10.1002/2013JD021043, 2014.